Approaching the pygmy dipole resonance in Sn isotopes with the Oslo method

Maria Markova[1,*], *Ann-Cecilie* Larsen[1], and *Frank Leonel* Bello Garrote[1]

[1]Department of Physics, University of Oslo, N-0316 Oslo, Norway

Abstract. The γ-ray strength functions (GSF) and nuclear level densities (NLD) below the neutron separation energy were extracted for $^{111-113,116-122,124}$Sn from particle-γ coincidence data with the Oslo method in a model consistent way. Combined with results of a recent systematic Coulomb excitation study, the Oslo GSFs were used to extract bulk characteristics of the low-lying electric dipole response, commonly associated with the pygmy dipole resonance (PDR). A resonance-like peak on top of the tail of the isovector giant dipole resonance was observed in all of the isotopes. It is centered at ≈8 MeV and exhausts ≈2% of the classical Thomas-Reiche-Kuhn (TRK) sum. For the heaviest isotopes, the data suggest also a second peak located at ≈6.5 MeV, which might potentially be the isovector component of the PDR. At variance with microscopic calculations, no clear increase of the total low-lying $E1$ strength with neutron excess was observed in the experimental data. The results also suggest that association of the full low-lying electric dipole strength with the PDR, especially in its neutron skin interpretation, might be unfounded.

1 Introduction

The pygmy dipole resonance (PDR) is commonly identified with a resonance-like enhancement in the electric dipole response of heavy nuclei around the neutron threshold. While its true nature, properties, and experimental signatures still remain a highly debated topic, numerous theoretical studies favor the neutron skin oscillation origin of the PDR [1]. In this interpretation, its strength is expected to be correlated with the neutron excess and, potentially, the neutron skin thickness, which might provide useful constraints for the symmetry energy parameters of the equation of state for neutron-rich matter [2]. Moreover, the presence of a large PDR strength in the nuclear response below the neutron separation energy has been suggested to impact the cross sections of (n,γ) reactions relevant for the heavy element nucleosynthesis [3].

Despite numerous experimental studies using complementary probes, consistent systematic experimental information on the evolution of the PDR in isotopic chains is quite scanty. Moreover, due to experimental limitations, parts of the low-lying $E1$ strength might be unavailable, additionally complicating a direct comparison of different experimental results and theoretical calculations. The Oslo method is commonly used to extract the statistical properties of nuclei, such as nuclear level densities (NLD) and γ ray strength functions (GSF), corresponding to the complete dipole response below the neutron threshold [4]. Here we present a systematic study of the low-lying electric dipole response (LEDR) in $Z = 50$ Sn isotopes with mass numbers ranging from $A = 111$ to 124 using the Oslo method. It allows us to investigate the evolution of this strength and, presumably, the PDR with gradually increasing proton-neutron asymmetry.

*e-mail: maria.markova@fys.uio.no

2 Experiments and the Oslo method

2.1 Experimental details and methodology

Eleven tin isotopes ($^{111-113,116-122,124}$Sn) were studied using light-particle-induced reactions with p, d, and ^{3}He beams in several experimental campaigns at the Oslo Cyclotron Laboratory (OCL). All experiments before 2018 were performed using the CACTUS γ ball, consisting of 28 5″ × 5″ NaI(Tl) detectors. A new scintillator detector array OSCAR, made of 30 large-volume $LaBr_3$(Ce) crystals, replaced the CACTUS array in the most recent experiments, providing significantly improved energy resolution and timing conditions. Outgoing particles were detected by a custom-designed Si telescope ring (SiRi), made of eight 1500-μm-thick E and 64 segments of ≈140-μm-thick ΔE counters. Particle angles covered by SiRi ranged from 40° to 54° for the earliest experiments (forward position) and from 126° to 140° for the latest experiments (backward position). The excitation energy resolution achieved in these experiments is ≈ 100−300 keV, depending primarily on the target thickness and the particle beam used. The ^{112,117,119,120,122,124}Sn targets were studied in the (p,p'), (p,d), (d,p), (^{3}He, ^{3}He′), and (^{3}He, α) reactions with 16 and 25 MeV protons, 11.5 MeV deuterons, and a 38 MeV ^{3}He beam. The energy deposited in the particle detectors was converted into the initial excitation energy E_i of the residual nucleus for the further analysis. A more detailed description of experimental conditions and procedures is outlined in [5].

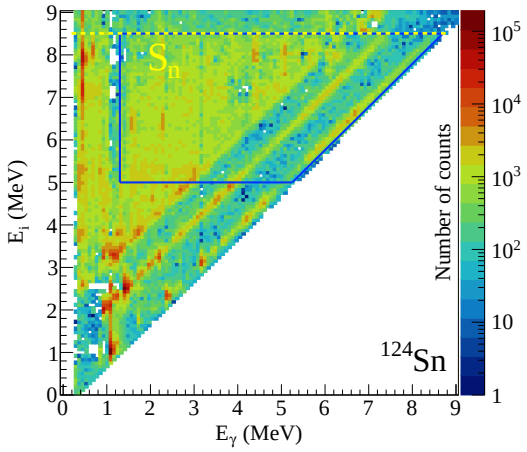

Figure 1. The first-generation matrix for ^{124}Sn extracted in the $(p, p'\gamma)$ experiment. The yellow dashed line corresponds to the neutron separation energy, while the blue solid lines confine the area used for the Oslo method. The bin size is 80 keV×80 keV.

These configurations of the experimental setup were used to extract particle-γ coincidence data in the form of γ ray spectra, corresponding to excitation energies of the studied nuclei up to their respective neutron separation energies (S_n). These spectra were unfolded using the CACTUS and OSCAR detector responses. Further, all second and higher order transitions in the observed γ cascades were removed by applying the iterative first-generation method, presented in great detail in Ref. [4]. Due to the limitation of this procedure, the data are usually available for $E_\gamma \gtrsim 1-2$ MeV and initial excitation energies from $3-5$ MeV to S_n. An example of the so-called first-generation matrix used as the main input for the Oslo method is shown in Fig. 1 for ^{124}Sn.

The principal idea of the Oslo method implies a decomposition of the first generation matrix $P(E_\gamma, E_i)$ into the γ transmission coefficient $\mathcal{T}_{i\to f}$ and the density of final levels ρ_f:

$$P(E_\gamma, E_i) \propto \mathcal{T}_{i\to f} \cdot \rho_f. \quad (1)$$

Being valid only for compound excited states, this relation is expected to hold well for the chosen excitation-energy ranges. Assuming the Brink-Axel hypothesis, which has been shown to be applicable for Sn isotopes [6], the decomposition results in the functional forms of the NLD and GSF, proportional to the γ transmission coefficient. External experimental data are required to normalize the decomposed solutions. This is commonly done by extracting the slope of the NLD and GSF from the experimental value of the average neutron resonance spacing, adjusting the absolute values of the NLD to the low-lying tabulated discrete states, and constraining the absolute values of the GSF with the average total radiative width from neutron resonance studies. The choice of normalization parameters, their values, and other details of this procedure are provided in [5].

2.2 Nuclear level densities and γ ray strength functions of Sn isotopes

The NLDs of $^{111-113,116-122,124}$Sn extracted in a model consistent way using the Oslo method are shown in Fig. 2. As expected for nuclei with quite similar structural properties, the densities of even-even isotopes agree nicely with each other. Similarly, the NLDs of even-odd isotopes are in good agreement, being on average 4-8 times higher than for the even-even neighbors due to the presence of an unpaired neutron. All NLDs reproduce available low-lying discrete states well up to ≈ 3 MeV and demonstrate a clear constant-temperature trend toward the neutron thresholds.

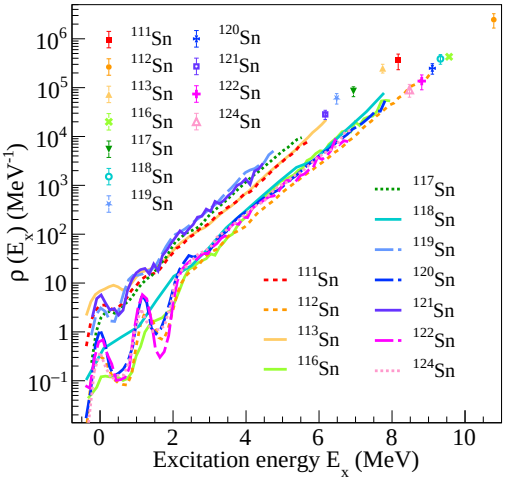

Figure 2. Experimental NLDs for $^{111-113,116-122,124}$Sn extracted with the Oslo method. The uncertainty bands are omitted for enhancing the clarity of the figure.

The GSFs of the studied nuclei are shown together in Fig. 3, separated by a common factor to reveal the evolution of the slope with increasing neutron number more clearly. All of the strengths point at a presence of an enhancement at ≈ 8 MeV, interpreted as a candidate for the PDR in the earlier works [5]. Albeit quite similar in shape, the GSFs demonstrate a mild increase of the slope with increasing neutron number, making the 8-MeV enhancement particularly pronounced for ^{124}Sn. As shown in Ref. [5], the strengths agree well within the experimental uncertainties with GSFs from relativistic Coulomb excitation in forward-angle (p, p') scattering [7] and (γ, n) data above the neutron threshold. This agreement additionally supports the normalization of the Oslo results.

3 Systematics of the low-lying $E1$ strength

3.1 Decomposition of experimental data

The Oslo method does not distinguish between electric and magnetic types of transitions, therefore, the GSFs presented in Fig. 3 include both the dominant $E1$ and $M1$ components. To access the LEDR, the following contributions to the total dipole strength should be considered: a low-energy tail of the isovector giant dipole resonance

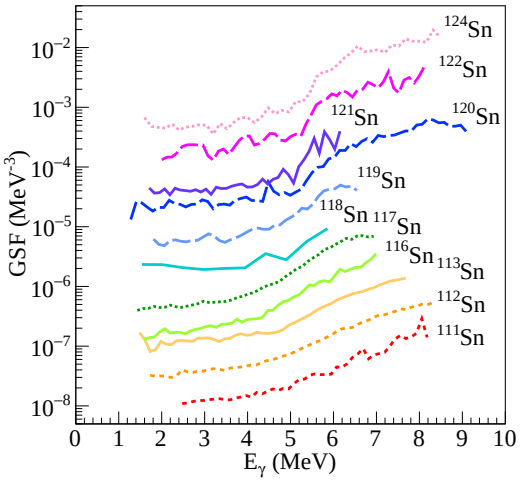

Figure 3. Experimental GSFs for $^{111-113,116-122,124}$Sn extracted with the Oslo method. The GSFs are separated by a constant factor of three (the strength of ^{111}Sn is not scaled). The uncertainty bands are omitted.

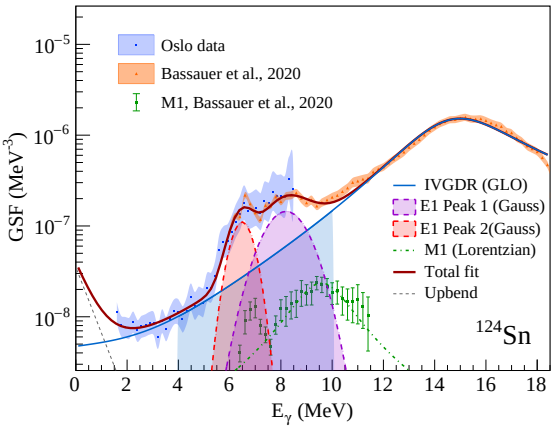

Figure 4. Decomposition of the experimental GSF of ^{124}Sn. The Oslo data (blue data points and the error band) are shown together with the (p, p') results (orange data points and the error band) [7]. The fit of the IVGDR is presented as solid blue line. The low-lying $E1$ components are shown as shaded red and violet areas. The $M1$ data from the (p, p') experiment [7] and the corresponding Lorentzian fit are given by the green data points and the dashed line, respectively. The upbend at low γ energies is described by the grey dashed line. The total fit is shown as the solid magenta line.

(IVGDR), a spin-flip $M1$ resonance, an upbend at very low energies (if present), and one or several (when demanded by the data) low-lying $E1$ features. To perform such a decomposition, the Oslo method results were combined with the dipole (p, p') GSFs for even-even stable isotopes, available in an energy range 6 – 20 MeV, thus covering the major part of the IVGDR. Data on the $M1$ spin-flip resonance are also available from the same series of the (p, p') experiments. A simple Lorentzian shape was assumed to parametrize the $M1$ data in even-even isotopes. The $M1$ resonance parameters in odd isotopes were consequently extracted using the even-even isotope systematics. A more detailed fit of the experimental $M1$ data does not impact the results in any significant way.

The generalized Lorentzian model was chosen to describe the IVGDR part, capable of accounting simultaneously for the low-energy flank of the IVGDR and a relatively flat strength distribution at very low energies (2 – 4 MeV), in contrast to other empirical and microscopic models. An exponential function was used to complete the fit at low energies (below 2 MeV). Since no clear upbend was observed in Sn isotopes, inclusion or exclusion of this feature does not affect the decomposition at higher energies. An enhancement at $\approx$ 8 MeV is well reproduced by a single Gaussian function in the lightest studied isotopes. The (p, p') data and a somewhat steeper slope of the Oslo method GSF in the isotopes with the mass number $A \geq 118$ require a second Gaussian resonance for an improved fit below S_n. An example of the decomposition of the total GSF is shown in Fig. 4 for ^{124}Sn. A more detailed discussion of this procedure and all fit parameters are provided in Ref. [5].

3.2 Discussion

Figure 5(a) presents the evolution of the LEDR in terms of the classical Thomas-Reiche-Kuhn (TRK) sum rule values (estimated as $60NZ/A$ MeV·mb for each isotope) exhausted by it. The strength in the Gaussian peaks is shown together with the total $E1$ strength, integrated within the 4 – 10 MeV energy range, and the strength within the tail of the IVGDR in the same region. The total LEDR is roughly constant (with slight indications of a local maximum at ^{120}Sn) with values ranging from 3.5% to 4.5% of the TRK sum rule. Similarly, the contribution of the low-energy tail of the IVGDR is approximately constant throughout the whole chain of the studied isotopes, exhausting a TRK value of about 1.5%. The dominant peak is centered at about 8.3 MeV and its average strength is $\approx$ 2% of the TRK value. As shown in Fig. 5(b), the smaller peak remains at $\approx$ 6.5 MeV in the heaviest isotopes. Interestingly, its strength depends nearly linearly on neutron number and reaches the maximum value of 0.5% for ^{124}Sn. Studies of the isoscalar $E1$ strength in ^{124}Sn with the $(\alpha, \alpha'\gamma)$ and (^{17}O,^{17} O$'\gamma$) reactions (see [8] and references therein) show a concentration of the $E1$ strength between 5.5 and 7 MeV, consistent with the properties of the observed lower-energy peak. Furthermore, studies of the ^{112,116,120,124}Sn(γ, γ') reaction ([5] and references therein) find the strongest transitions in the same energy region, indicating large ground state branching ratios. These experiments suggest that the observed lower-energy peak might potentially be a candidate for the isovector response of the PDR.

The observed trend in the evolution of the LEDR with increasing neutron number largely disagrees with the vast majority of theoretical predictions. For example, calculations within the microscopic relativistic quasiparticle random-phase and time-blocking approximations (RQRPA and RQTBA) demonstrate a clearly increas-

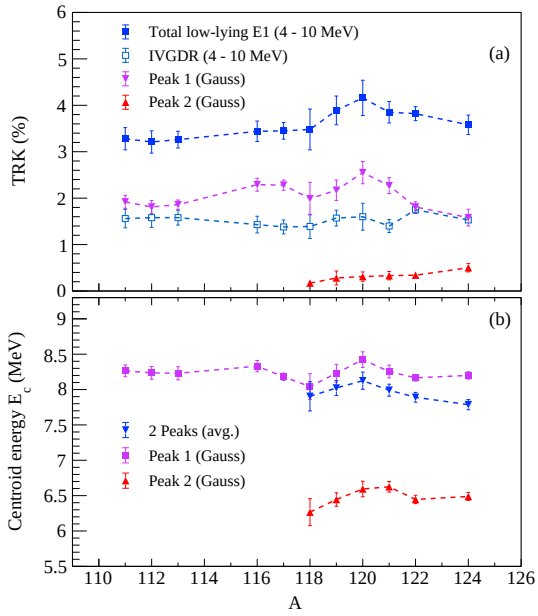

Figure 5. Systematics of the total LEDR in the energy region from 4 to 10 MeV and its decompostion into the contributions from the tail of the IVGDR and one or two (for masses $\geq$ 118) resonances on top. (a) Energy-weighted integrated strengths in % of the corresponding TRK sum rule values for each isotope. (b) Centroid energies.

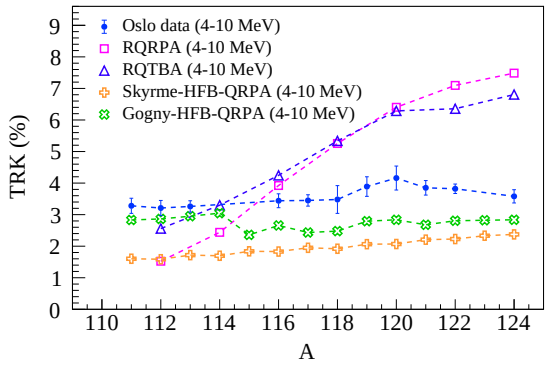

Figure 6. Evolution of the experimental LEDR in the energy range of 4 – 10 MeV compared with predictions of the RQRPA (open squares) and RQTBA (open triangles) calculations. The Hartree-Fock-Bogolubov plus QRPA calculations using the BSk7 Skyrme force (orange open pluses) and the D1M Gogny force (green open crosses) are also shown (see [9] and references therein). The dashed lines are added to guide the eye.

ing low-lying $E1$ strength with increasing proton-neutron asymmetry (see [5] for details). Figure 6 shows a fraction of the TRK sum rule exhausted by the RQRPA, RQTBA, and the experimental strength in the 4 – 10 MeV energy interval. Due to an improved fragmentation of the strength as compared with RQRPA, RQTBA reproduces an overall shape of the experimental LEDR fairly well. However, it still significantly overestimates the amount of the experimentally observed strength in this energy range, especially in the heaviest stable isotopes. On the contrary, non-relativistic approaches (see Fig. 6) provide a somewhat better agreement with the Oslo data in the exhausted TRK values and the general trend with increasing neutron number, albeit still failing to capture the experimental enhancement of the strength at $\approx$ 8 MeV.

4 Conclusions

The low-lying electric dipole strength has been extracted in a model-consistent way with the Oslo method for eleven Sn isotopes in order to study its evolution with increasing neutron excess. Combining these data below the neutron threshold with the results of the relativistic Coulomb excitation experiment allows us to extract the bulk characteristics of a resonance-like feature at $\approx$ 8 MeV, observed in all cases. It was found to exhaust an approximately constant fraction of the TRK sum rule which does not exceed 2 – 3%. The total strength including the IVGDR contribution remains also nearly constant throughout the whole chain of isotopes. Based on the results of the earlier experiments with isoscalar and isovector probes, an additional low-lying $E1$ feature at 6.5 MeV in isotopes with $A \geq 118$ might be a potential candidate for the isovector component of the PDR. A small observed strength in this energy region challenges the neutron skin interpretation of the PDR. Finally, a direct comparison of the experimental data with RQRPA, RQTBA, Skyrme and Gogny HFB-QRPA calculations suggests further improvements in the theoretical description of the low-lying $E1$ strength.

References

[1] E. Lanza *et al.*, Prog. Part. Nucl. Phys. **129**, 104006 (2023). 10.1016/j.ppnp.2022.104006
[2] A. Klimkiewicz *et al.*, Phys. Rev. C **76**, 051603(R) (2007). 10.1103/PhysRevC.76.051603
[3] S. Goriely, Phys. Lett. B **436**, 10 (1998). 10.1016/S0370-2693(98)00907-1
[4] A. C. Larsen *et al.*, Phys. Rev. C **83**, 034315 (2011). 10.1103/PhysRevC.83.034315
[5] M. Markova *et al.*, Phys. Rev. C **109**, 054311 (2024). 10.1103/PhysRevC.109.054311
[6] M. Markova *et al.*, Phys. Rev. Lett. **127**, 182501 (2021). 10.1103/PhysRevLett.127.182501
[7] S. Bassauer *et al.*, Phys. Rev. C **102**, 034327 (2020). 10.1103/PhysRevC.102.034327
[8] L. Pellegri *et al.*, Phys. Lett. B **738**, 519 (2014). 10.1016/j.physletb.2014.08.029
[9] A. Koning *et al.*, Eur. Phys. J. A **59**, 131 (2023). 10.1140/epja/s10050-023-01034-3